Available online at www.sciencedirect.com
SCIENCE DIRECT®
Physica E 25 (2004) 303–312
PHYSICA E
www.elsevier.com/locate/physe

Quantum rings as phase coherent detectors

A. Fuhrer[a,*], M. Sigrist[a], L. Meier[a], T. Ihn[a], K. Ensslin[a], W. Wegscheider[b], M. Bichler[c]

[a] *Solid State Physics Laboratory, ETH Zurich, 8093 Zürich, Switzerland*
[b] *Institut für experimentelle und angewandte Physik, Universität Regensburg, Germany*
[c] *Walter Schottky Institut, Technische Universität München, Germany*

Available online 21 July 2004

Abstract

Aharonov–Bohm oscillations are studied in the magnetoconductance through two micron-sized quantum rings. The structures are defined in a two-dimensional electron gas of a Ga[Al]As heterostructure by way of local oxidation with an atomic force microscope. In the experiments, the rings are used as phase-coherent detectors of the charge state of quantum dots coupled to the rings in two specific arrangements.

In the first case, two quantum dots are induced in each of the arms of an open four-terminal ring geometry. This allows to measure the evolution of the relative transmission phase when the number of electrons in each of the dots is tuned using appropriate gate voltages. The experimental findings are compared to expectations from single-particle theory and deviations are discussed.

In the second case, a quantum dot is coupled capacitively to one arm of a ring. The amplitude of the Aharonov–Bohm oscillations in the transconductance depends strongly on the charge state of the quantum dot. It is demonstrated that the effect is due to a single-electron screening effect. This shows that Aharonov–Bohm oscillations in a quantum ring can be used for the detection of single electronic charges.

PACS: 73.23.Ad; 73.63.Kv

Keywords: Transmission phase; Quantum dot; Aharonov–Bohm effect; Phase coherence

1. Introduction

Mesoscopic rings and ring-like geometries allow the observation of the interference of partial waves as a function of magnetic field, i.e., the Aharonov–Bohm (AB) effect [1–4]. Such measurements yield information about electron decoherence e.g. as a function of temperature [3,4]. Coupled mesoscopic systems are of interest for experimentalists trying to realize detectors of single charges, controlled interference and entanglement in semiconductor nanostructures. In the present paper, we review two of our experiments that investigate the coupling between quantum dots and mesoscopic ring structures. In these experiments, the influence of the charge state of the quantum dot on the phase-coherence in the ring is detected by

*Corresponding author. Tel.: +41-1-633-3769.
E-mail address: fuhrer@phys.ethz.ch (A. Fuhrer).

1386-9477/$ - see front matter
doi:10.1016/j.physe.2004.06.029

measuring AB-oscillations in the conductance through the ring.

The experiments are representative for two limiting cases of how coupling can be achieved. In one case, two mesoscopic systems are coupled simply by the electrostatic interaction between them without the overlap of wavefunctions of the systems to be coupled [5–9]. Such systems have been realized in a number of experiments, e.g. quantum point contacts have been employed as non-invasive probes to detect the charge state of single or double quantum dots and antidots by way of electrostatic interaction between the two systems [10–17]. Mesoscopic detectors such as quantum point contacts situated close to another quantum system are expected to lead to dephasing [5,6]. In a ring this will reduce the amplitude of the phase coherent AB oscillations. Such a 'which path' experiment has been realized by Buks and coworkers, who coupled a quantum dot embedded in one arm of an AB interferometer electrostatically to a quantum point contact [18]. Another experiment investigated the coupling between edge states in the quantum Hall regime and a double quantum dot system [13].

In the other limiting case, the coupling is realized by strong wavefunction overlap and the electrostatic interaction between the systems plays a minor role. Such systems have been studied, e.g., in strongly coupled double dots [19–21] and for quantum dots embedded in ring geometries [11,18,20–25]. The electronic transmission phase in particular was studied in a series of experiments [11,22–25] where ring geometries have been employed as interferometers, namely quantum dots were inserted in one arm of the ring. From measurements of the relative transmission phase through a two-terminal ring with a single quantum dot [22], it was concluded that electron transport through a Coulomb-blockaded quantum dot is at least partially phase coherent. However, such a two-terminal measurement will not allow to determine the evolution of the transmission phase due to the generalized Onsager relations [26] which state that the magnetoconductance in such a device is an even function of magnetic field restricting the phase to values of 0 or π. To circumvent this problem multi-terminal rings were investigated in subsequent experiments [11,18,23,24]. It was found that the relative transmission phase of such a ring changes by π when the embedded quantum dot is tuned over a Coulomb blockade resonance. Between resonances, it is frequently observed that the so-called phase lapses occur rather than the almost constant phase expected in the simplest model. For a review of the theoretical work on this subject see Ref. [27].

In our experiments, we study the coupling between a ring and a dot in each of the two limits discussed above. We start out by investigating the phase evolution of a system of two quantum dots with negligible electrostatic interaction between them, embedded in two arms of a four-terminal AB ring. Unlike previous experiments, we are able to tune the number of electrons in each of the dots individually while detecting changes in the phase of the AB oscillations. The measurements are performed in an intermediate coupling regime where the amplitude of the AB oscillations is large enough for our analysis. Furthermore, we discuss a situation in the opposite limit of pure electrostatic coupling where a dot is placed adjacent to one of the rings arms. Although, from the quantum measurement point of view, in such an arrangement the quantum dot could be regarded as a 'which path detector' for electrons traversing the quantum ring, it is argued that the observed reduction of the AB oscillation amplitude in the transconductance is not due to dephasing but rather a single electron screening effect.

2. The ring samples

The coupled ring-dot structures were realized in a Ga[Al]As heterostructure with a two-dimensional electron gas, 37 nm below the surface. The lateral patterns were fabricated with the biased tip of an atomic force microscope which locally oxidizes the GaAs surface. Details of this fabrication technique are described in Ref. [28]. Figs. 1(a) and (b) show micrographs of the oxidized patterns. Lateral gate electrodes marked pg1 through pg4 are used to tune the conductance and electron number of the quantum dots. All measurements

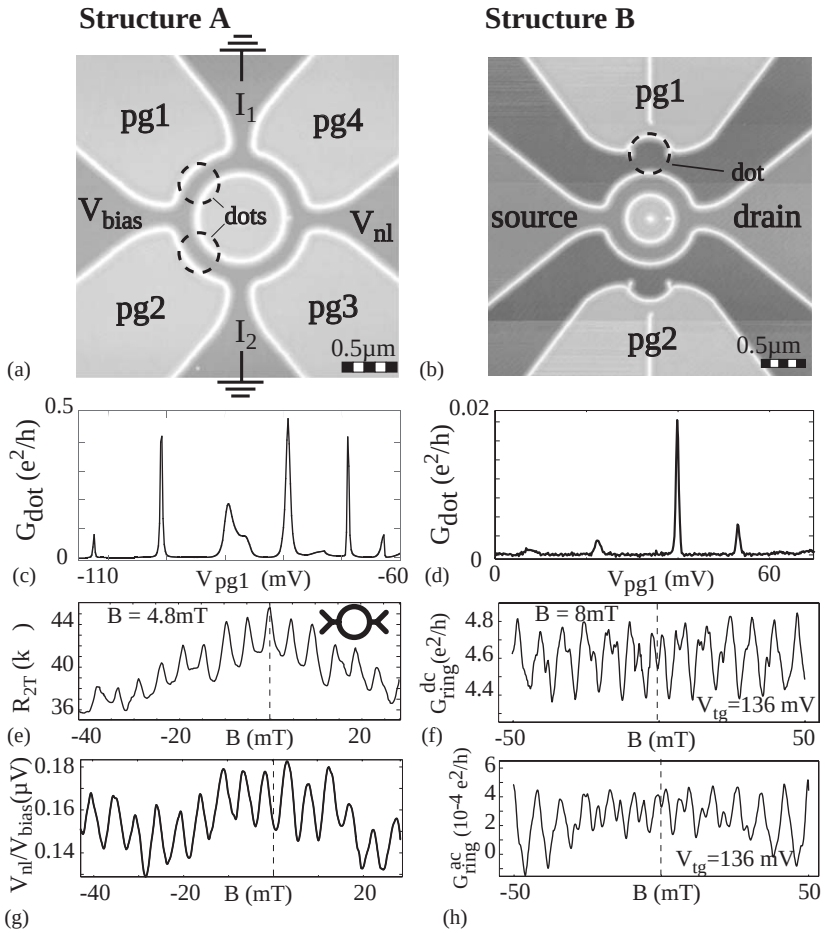

Fig. 1. (a,b) AFM micrographs of the two ring structures. The oxide lines (bright lines) written by local oxidation with an AFM tip lead to insulating barriers in the two-dimensional electron gas, 37 nm below the surface. The areas marked pg1–pg4 are used as lateral gates to tune the conductance of the four arms of the ring and act as plunger gates for the dots. In two-terminal measurements, a fixed current is passed from source to drain and the voltage drop across the ring is measured. In the four-terminal arrangement, a voltage bias of $V_{bias} = 16\,\mu V$ is applied on the left and the non-local voltage V_{nl} is measured. Two additional leads (top and bottom) are connected to ground and the currents I_1, I_2 close to the corresponding dots are measured. (c,d) Coulomb blockade oscillations in the quantum dots (dashed circles) as a function of a voltage applied to the gate. For 'structure A' a dot was induced in the segment of the ring adjacent to plunger gate pg1 by applying negative gate voltages. One of the other segments was pinched off during the measurement in order to prevent current flow parallel to the dot. (e,f) Two-terminal measurements of the Aharonov–Bohm (AB) effect in the the resistance and conductance of the rings, respectively. (g) AB-oscillations in the non-local voltage V_{nl}. (h) AB-oscillations in the transconductance of the ring.

were carried out in a dilution refrigerator with a base temperature of 40 mK.

Figs. 1(c) and (d) show pronounced conductance oscillations in the quantum dots [dashed circles in Figs. 1(a) and (b)] when measured individually. While the tunnel barriers of the dot in 'structure B' were explicitly defined by writing two short oxide lines, the dots in 'structure A' were induced through negative gate voltages applied to the corresponding in-plane gate electrode [29].

The rings were characterized in two-terminal measurements in the open regime and pronounced AB oscillations are found [see Figs. 1(e) and (f)]. The period of the AB oscillation is $\Delta B = 4.8$ and 8 mT for structure A and B, respectively, and directly reflects the different size of the two rings.

We find small deviations (<10% of the total signal) from a perfect symmetry around zero magnetic field (dashed line) as required by the Onsager relations. From temperature-dependent measurements of the AB effect on an even smaller ring [4], we estimate that the phase-coherence length in these samples at $T = 100$ mK is larger than 10 μm and therefore persists outside the ring structure. This could explain the observed deviations since the measurements outside the ring structure itself were performed in a four terminal configuration as indicated in the inset of Fig. 1(e). The ring conductance in 'structure B' at small magnetic field values shows oscillations with multiples of the AB frequency, indicating that paths which circle the ring at least once before interfering are of importance in the smaller ring. Generally, we can express the conductance of the ring with area A in a magnetic field B as

$$G^{dc}_{\mathrm{ring}}(V^{dc}_{\mathrm{pg}}, B) = G^{dc}_{0}(V^{dc}_{\mathrm{pg}}) + G^{dc}_{1}(V^{dc}_{\mathrm{pg}})\cos\left(2\pi\frac{BA}{h/e} + \delta_1\right) + \cdots, \quad (1)$$

where $G^{dc}_{1}(V^{dc}_{\mathrm{pg}})$ is the amplitude of the AB oscillations.

A true four-terminal measurement of the AB-effect is shown in Fig. 1(g) in the open regime of the ring in 'structure A' where each quadrant supports 2–4 lateral modes. In this configuration, a bias voltage V_{bias} was applied to the ring while upper and lower contacts were grounded using current–voltage converters to measure the currents I_1 and I_2 [see Fig. 1(a)]. The non-local voltage V_{nl} was detected at the contact on the right. While the period is the same as for the two-terminal measurement there is clearly no symmetry around zero magnetic field in this case. Also, this configuration allows for a much larger signal-to-noise ratio than the corresponding local measurement.

3. Transmission phase

We proceed to discuss the influence of Coulomb charging of the dots in 'structure A' on the phase of the AB-oscillations detected in the non-local voltage. The measurements are performed in the configuration shown in Fig. 1(a) where two dots are induced in segments 1 and 2 of the ring and segments 3 and 4 are open. Fig. 2(a) shows a grayscale image of the non-local voltage V_{nl} as a function of the voltages applied to each of the two plunger gates pg1 and pg2 of the quantum dots. In the weak coupling regime for strongly negative gate voltages we observe well defined peaks with two characteristic slopes indicating

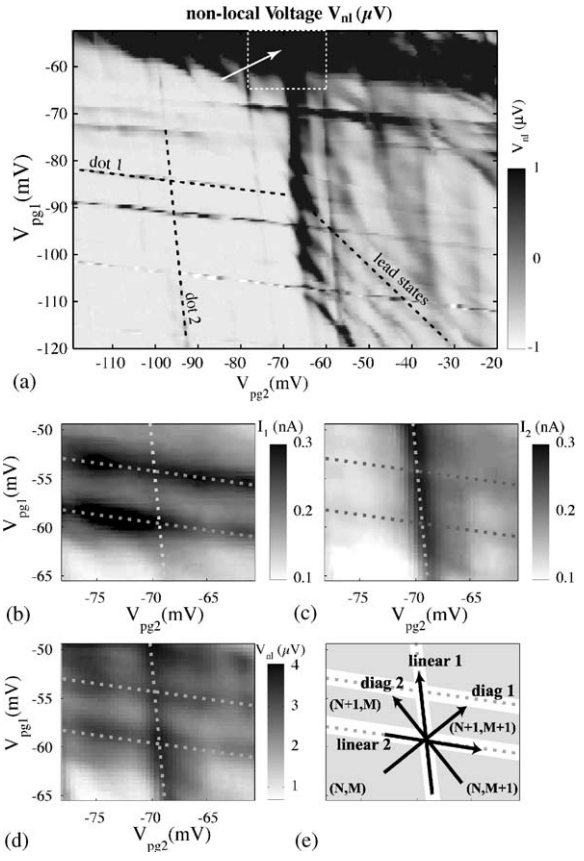

Fig. 2. (a) Grayscale image of the non-local voltage V_{nl} as a function of the voltage applied to each of the two plunger gates pg1,pg2 of the quantum dots. The dashed lines indicate the evolution of Coulomb resonances in each of the dots and resonances in the ring area between the two dots. The Aharonov–Bohm measurements were performed in the shaded area where two conductance peaks of dot1 cross a conductance peak of dot2. The figures below show close-ups in this regime of the three measured values, namely the currents (b) I_1 and (c) I_2 and the non-local voltage (d) V_{nl}. (e) Schematic drawing of the peaks positions and the gate-sweeps discussed in the text.

Coulomb-blockade oscillations in each of the two dots (dashed lines). From measurements of Coulomb-blockade diamonds in each dot we extract the lever arms $\alpha_G \approx 0.16$ of the gate closest to the corresponding dot [30] and find a typical charging energy of 1 meV. The lever arm to the adjacent gates can be extracted from the slope of the dashed lines in Fig. 1(a) and is a factor of six smaller. For the gate opposite the corresponding dot the lever arm is 14 times smaller. The peaks in this weak coupling regime are narrow and we conclude that there is negligible electrostatic interaction between the dots from the fact that the peaks cross each other with no observable shifts or splitting as expected e.g. for a double quantum dot with electrostatic coupling [31]. However, in this regime it was not possible to detect AB oscillations as a function of magnetic field. Therefore, we performed our measurements in an intermediate coupling regime (see arrow in Fig. 2(a)) where both the AB signal was strong enough and the Coulomb resonances were still well defined. We focus on a parameter range where two Coulomb resonances in each of the dots cross each other. This is shown in measurements of the two currents I_1 and I_2 in Figs. 2(b) and (c), respectively, where the resonance in the dot closer to the corresponding current lead shows up much more strongly. Fig. 2(d) shows a zoom of the non-local voltage, which for the same parameter range, displays clear signatures of conductance resonances of both quantum dots. The Coulomb resonances are indicated by the dashed lines and the schematic drawing in Fig. 2(e) shows how the electron configuration in the dots can be tuned along selected gate voltage sweeps indicated by the black arrows.

In order to study the phase evolution of the transmission through the quantum dots, we now proceed to measure V_{nl} as a function of magnetic field and for gate voltages along the arrow 'linear 2' indicated in Fig. 2(e), where we stay on a conductance maximum of dot 1 while dot 2 is tuned over a Coulomb resonance. Fig. 3(a) shows a grayscale image of the AB oscillations in V_{nl} as a function of V_{pg2}. The AB oscillations are strongest in the range of the conductance maximum indicated by the dashed line. Fig. 3(b) shows

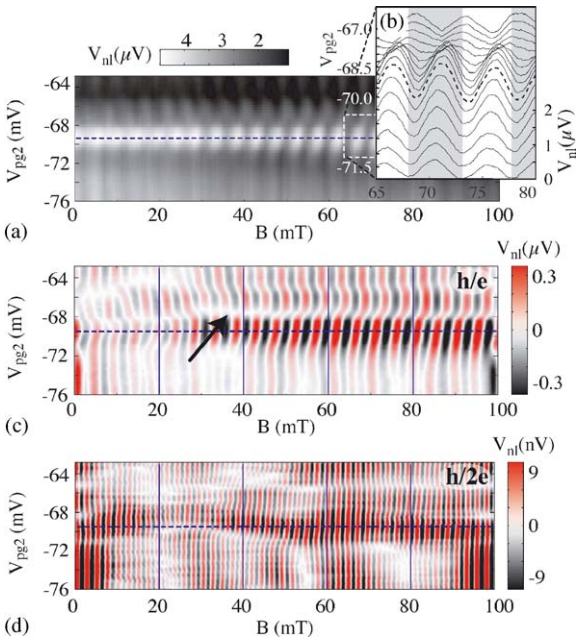

Fig. 3. (a) Gray scale image of Aharonov–Bohm oscillations in the non-local voltage as a function of the gate voltages tuned along 'linear2' across a conductance resonance in dot 2 while keeping dot 1 on a conductance maximum. (b) shows individual traces in a selected magnetic field range (indicated by the white dashed rectangle) and gate voltages close to the conductance peak. The phase increases by about π. Curves have been offset by 0.3 μV for clarity. (c) h/e periodic contribution to the non-local voltage extracted from the raw data by applying the filter function to the Fourier transformed data as outlined in the text (d) $h/2e$ periodic contribution extracted by a similar procedure.

individual magnetic field traces in a range where dot 2 is tuned over the Coulomb resonance. A phase shift of about π can be directly observed compatible with expectation from straightforward theory [27].

To analyze such phase shifts more quantitatively, the fast Fourier transform of each magnetic field sweep was multiplied with the filter function $f(\omega) = (\sigma\omega)^2/2 \exp[1 - (\sigma\omega)^2/2]$ with $\sigma = \Delta B/\sqrt{2}\pi$ in order to obtain the pure h/e-periodic contribution. The inverse fast Fourier transform of the filtered data gives the oscillatory component of V_{nl} as a function of magnetic field which is plotted in Fig. 3(c). The same procedure was also done for the $h/2e$ periodic component of V_{nl} as shown in Fig. 3(d). However, the $h/2e$ oscillation amplitude in this ring was about a

factor 30 smaller and the peak in the Fourier spectrum was only just detectable. This indicates that paths which go around the ring several times are suppressed in the multi-terminal configuration used in our setup as expected.

From Fig. 3(c) we find that while the qualitative evolution of phase and amplitude of the AB oscillations is as expected, there is also a B-dependence, e.g. the amplitude on the peak increases with magnetic field and there are phase lapses in certain magnetic field regimes. Such a phase lapse occurs for example at the tip of the arrow in Fig. 3(c). This phase lapse lies in the flank of the Coulomb resonance and occurs only over a limited range of magnetic field. Beyond this field range the phase lapse disappears in favor of a continuous phase evolution of order π. A more detailed description of this behavior will be discussed elsewhere [32]. Here, we want to restrict ourselves to a qualitative analysis in the regime $40\ \mathrm{mT} < B < 70\ \mathrm{mT}$, where the phase behavior is fairly regular for all the gate sweeps along the arrows shown in Fig. 2(e). For this purpose, we use a Fourier analysis to extract both the magnetic field averaged phase and amplitude as a function of gate voltage for each of the gate sweeps.

Fig. 4(a) shows the result for the sweep discussed above along trace 'linear 2' where an electron is added to dot 2 and indeed we find a phase change of about π as expected. However, when we measure along trace 'linear1' (Fig. 4(b)) where electrons are added to dot 1 we pass two resonances. The total phase shift is still about π but the phase shifts by $\pi/2$ for each of the peaks. Similar behavior has been observed for a dot in the Kondo regime [24,25]. The overall trend of the phase shift differs in sign from that along 'linear 2', in agreement with the fact that we tune the dot in the other interferometer arm. Along trace 'diag1' (Fig. 4(c)), an electron is added to both dots at the same time. In this case, a very small phase shift is found since the relative phase between the arms of the ring does not change. Along trace 'diag2' (Fig. 4(d)) an electron is removed from dot 2 and added to dot 1. As expected, AB oscillation maxima shifts in the same direction as in 'linear1'. However, the total phase change is only slightly more than π rather than the expected shift of 2π.

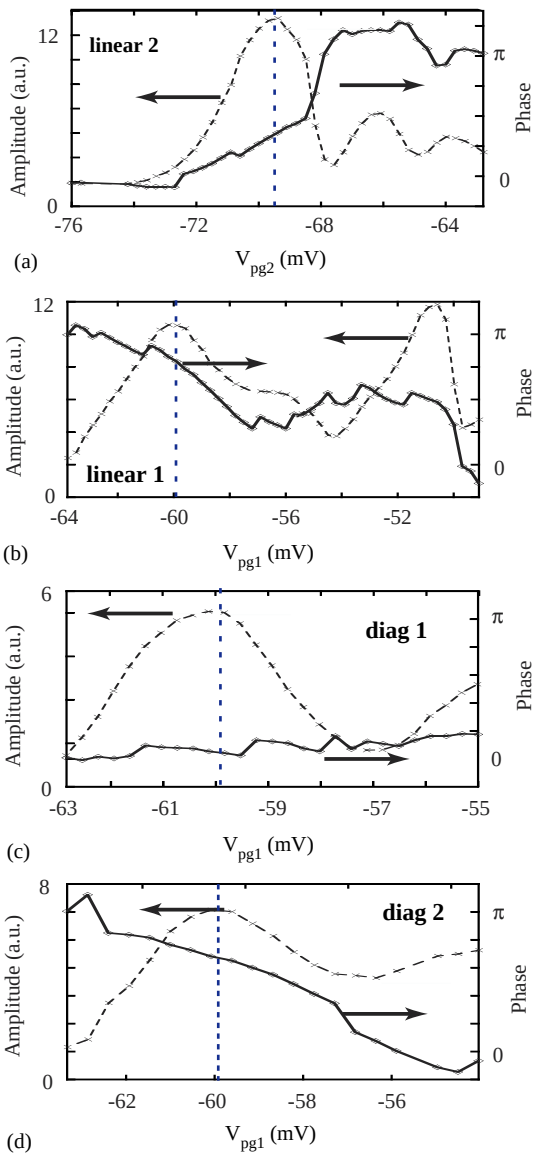

Fig. 4. Averaged phase and amplitude change of the AB-oscillations along selected sections of the sweeps discussed in the text close to the crossing of the Coulomb peaks in the V_{pg1}–V_{pg2} plane. The values shown were determined from Fourier analysis of the magnetic field range from 40 to 70 mT.

Summarizing our results on the transmission phase of two dots embedded in the arms of a ring interferometer, we can state that we have succeeded in measuring the AB phase in the intermediate coupling regime of the dots where

the AB oscillations are well developed and suitable for phase measurements. In the range between 40 and 70 mT the expected phase shifts across Coulomb-blockade resonances are qualitatively observed. However, we also find phase lapses that occur in finite magnetic field ranges at specific gate voltages which influence the quantitative measurement of the phase. A conceivable origin of the phase lapses is the finite width of the ring segments accommodating several modes. Furthermore, as the coupling increases with increasing V_{pg2} additional resonances appear with a diagonal behavior [dashed line 'lead states' in Fig. 2(a)]. From the relative slope to the two plunger gates, we find that these resonances must originate either in additional states that form in the left lead of the ring where the bias is applied or from the coherent coupling of the two dots. This together with the observed phase evolution in trace 'linear 1' may indicate that coherent processes between the two dots and the leads are of some importance. In such a case, the question arises how the transmission phases of individual resonances combine to the observed phase shift.

4. Single electron detection

Let us now turn to the second ring-dot system in 'structure B' where the coupling between the two is purely electrostatic. For the experiment described in the following, only one dot is important [dashed circle in Fig. 1(b)] and also the point contacts next to the quantum dots were not used. In this sample, the whole structure was covered by a metallic top gate giving additional tunability. The aim of the experiment was to study the influence of the charging of the quantum dot on the coherent part of the current through the ring. Again, we performed magnetoconductance measurements on the ring while stepping the gate voltage V_{pg1} on the dot. We determine the Fourier coefficients of the conductance of which we plot the constant part G_0^{dc} (see Eq. (1)) and the oscillatory part G_1^{dc} in Fig. 5(a) together with the conductance of the dot measured separately. We find that both G_0^{dc} and the AB signal depend on the gate voltage which modifies the symmetry of the ring [33]. However, to resolve features which are related to the charging of the dot, the resolution in this measurement is clearly not good enough. We therefore also measured AB oscillations in the transconductance $\mathrm{d}G_{ring}/\mathrm{d}V_{pg} = \mathrm{d}(I_{ring}/V_{bias})/\mathrm{d}V_{pg}^{(AC)}$, where I_{ring} is the current through the ring. This quantity is measured with lock-in techniques by applying a DC bias voltage V_{bias} between source and drain and modulating the plunger gate with $V_{pg}^{(AC)}$ at a frequency of 89 Hz. The modulation of the current through the ring is then detected at the same frequency. Fig. 1(h) shows an example of the resulting AB-oscillations in the transconductance. Fig. 5(b) displays the resulting curves which are a direct measurement of the derivative of the corresponding quantities in Fig. 5(a). In these measurements, dips can be detected that are correlated with the occurrence of peaks in the dot conductance (see dashed vertical lines). Note that the current through the dot was plotted on a logarithmic scale in Fig. 5(a).

To substantiate this, we show a more detailed measurement of the dip and the corresponding Coulomb peak in the inset in Fig. 6(a). The main figure shows the evolution of the Coulomb peak when the remote gate V_{pg2} is tuned which can be compared to the corresponding measurement of G_1^{dc} in Fig. 6(b) where the dip moves in exactly the same way. Note that when the quantum dot is conducting, the amplitude of the Aharonov–Bohm oscillations in the transconductance is found to be significantly suppressed by up to 40% as compared to the situation where the dot is blockaded.

Our interpretation of the reduced AB-amplitude involves screening of the modulated plunger gate voltage felt in the ring by single-electron charging in the dot on a conductance peak. The screening effect can be readily understood in a capacitive model (inset Fig. 6(b)). There is a direct capacitive coupling C_{rg} between plunger gate and ring arm. In addition, the capacitances between gate and dot, C_{dg} and dot and ring, C_{dr} are connected in series, parallel to C_{rg}. The induced charge on the arm of the ring is given by

$$Q_{ring} = \left[\left(\frac{1}{C_{dr}} + \frac{1}{C_{dg}}\right)^{-1} + C_{rg}\right] V_{pg}^{(DC)} + \frac{C_{dr}}{C_{dd}} Q_{dot}.$$

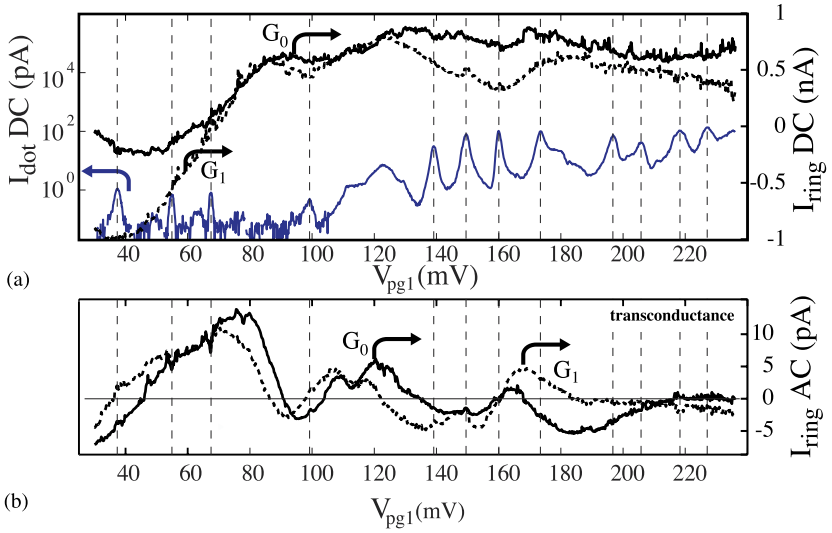

Fig. 5. (a) Dot current and Fourier coefficients of the two-terminal conductance of the ring as a function of the gate voltage applied to the dot. (b) Fourier coefficients of the transconductance through the ring when the gate voltage V_{pg1} is modulated. Each curve is a measurement of the derivative of the corresponding curve in (a).

When the charge on the dot Q_{dot} changes by $-|e|$ on a conductance peak, Q_{ring} changes in a small step ΔQ_{ring}. When $V_{pg}^{(DC)}$ is swept over a conductance peak in the dot, the thermal smearing of the peak will also smear the step in Q_{ring}. It is reasonable to assume that the corresponding local potential change in the ring is $\Delta U_{ring} \propto \Delta Q_{ring}$. This step ΔU_{ring} will lead to a step in all the conductances G_i as a function of $V_{pg}^{(DC)}$. Since the transconductance measures the derivative of the conductance, the step-like behavior in G_0 and G_1 appears as a dip at a value of V_{pg} where a conductance peak occurs in the dot. A thorough discussion of this single-electron screening effect will be published elsewhere [34].

The strong suppression of the AB oscillation amplitude on a conductance peak suggests the straightforward interpretation of the effect as being due to dephasing of partial waves in the ring in the spirit of a 'which-path' experiment. When the quantum dot is in the Coulomb blockade, its electron number is fixed and no information can be carried away about whether an electron passed through the adjacent ring arm. Viewed from the perspective of the electrons in the quantum ring, there are no time-dependent fluctuations of the potential in the ring near the dot, since there are no charge fluctuations in the blockade. On the other hand, if the dot becomes conducting, its charge state does fluctuate in time and the resulting fluctuations of the local potential in the ring may dephase the electron partial waves.

However, we argue that such an interpretation, though very appealing, does not explain the magnitude of the observed AB-amplitude reduction. Since the dwell time of electrons in the quantum dot is significantly larger than the time an electron needs to traverse the ring arm from source to drain, the ring's electrons feel only a slow, quasistatic potential variation which is very inefficient in dephasing.

5. Summary

In conclusion, we have studied the coupling between a ring and a dot in two coupling configurations. We have demonstrated that the phase coherent AB oscillations in a quantum ring are sensitive to single electron charging of an adjacent electrostatically coupled quantum dot and the ring can be used as a detector of the dot's charge state. Furthermore, we measured the phase evolution of a system of two quantum dots with

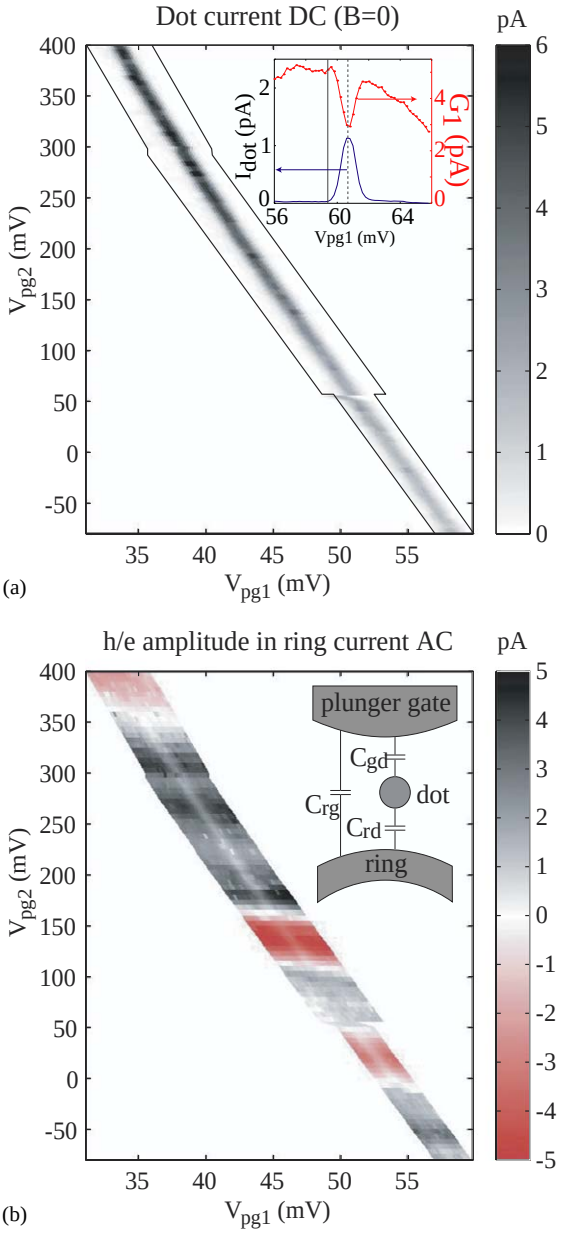

Fig. 6. (a) Gray scale image of the Coulomb peak in the dot current as a function of both plunger gate voltages. The inset shows how the Coulomb peak is correlated in position with the dip in transconductance. (b) Dip in the AB-signal of the transconductance which follows exactly the position of the Coulomb resonance shown in (a). The inset shows the capacitive model.

negligible electrostatic interaction embedded in two arms of a four-terminal AB ring. Here, we are able to tune the number of electrons in each of the dots individually while detecting changes in the phase of the AB oscillations. While the observed phase shifts, agree qualitatively with theoretical expectations, the phase evolution is found to depend also on the magnetic field and occasional phase lapses occur in limited magnetic field ranges that influence a quantitative analysis of the transmission phase of the dots. These observations highlight the need to consider non-local coherent effects in the entire system.

References

[1] Y. Aharonov, D. Bohm, Phys. Rev. 115 (1959) 485.
[2] G. Timp, A.M. Chang, J.E. Cunningham, T.Y. Chang, P. Mankiewich, R. Behringer, R.E. Howard, Phys. Rev. Lett. 58 (1987) 2814.
[3] A.E. Hansen, A. Kristensen, S. Pedersen, C.B. Soîrensen, P.E. Lindelof, Phys. Rev. B 64 (2001) 045327.
[4] T. Ihn, A. Fuhrer, M. Sigrist, K. Ensslin, W. Wegscheider, M. Bichler, Adv. Solid State Phys. 43 (2003) 139.
[5] Y. Levinson, Europhys. Lett. 39 (1997) 299.
[6] S.A. Gurvitz, Phys. Rev. B (1997) 15215.
[7] M. Büttiker, A. Martin, Phys. Rev. B 61 (2000) 2737.
[8] T. Pohjola, H. Schoeller, G. Schön, Europhys. Lett. 54 (2001) 241.
[9] S. Pilgram, M. Büttiker, Phys. Rev. Lett. 89 (2002) 200401.
[10] M. Field, C.G. Smith, M. Pepper, D.A. Richie, J.E.F. Frost, G.A.C. Jones, D.G. Hasko, Phys. Rev. Lett. 70 (1993) 1311.
[11] E. Bulks, R. Schuster, M. Heiblum, D. Mahalu, V. Umansky, Phys. Rev. Lett. 77 (1997) 4664.
[12] J. Cooper, C.G. Smith, D.A. Ritchie, E.H. Linfield, Y. Jin. H. Launois, Physica E 6 (2000) 457.
[13] D. Sprinzak, Y. Ji, M. Heiblum, D. Mahalu, H. Shtrikman, Phys. Rev. Lett. 88 (2002) 176805.
[14] C.G. Smith, S. Gardelis, J. Cooper, D.A. Ritchie, E.H. Linfield, Y. Jin, H. Launois, Physica E 12 (2002) 830.
[15] S. Gardelis, C. Smith, J. Cooper, D. Ritchie, E. Linefield, Y. Jin, H. Launois, Phys. Rev. B 67 (2003) 073302.
[16] J.M. Elzerman, R. Hanson, J.S. Greidanus, L.H.W. van Beveren, S.D. Franceschi, L.M.K. Vandersypen, S. Tarucha, L.P. Kouwenhoven, Phys. Rev. B 67 (2003) 161308(R).
[17] M. Kataoka, C.J.B. Ford, G. Faini, D. Mailly, M.Y. Simmons, D.R. Mace, C.T. Liang, D.A. Ritchie, Physica E 6 (2000) 495.
[18] E. Buks, R. Schuster, M. Heiblum, D. Mahalu, V. Umansky, Nature 391 (1998) 871.
[19] H. Jeong, A.M. Chang, M.R. Melloch, Science 293 (2001) 2221.

[20] A.W. Holleitner, C.R. Decker, H. Qin, K. Eberl, R.H. Blick, Phys. Rev. Lett. 87 (2001) 256802.
[21] A. Holleitner, C.R. Decker, H. Qin, K. Eberl, R.H. Blick, Science 297 (2002) 70.
[22] A. Yacoby, M. Heiblum, D. Mahalu, H. Shtrikman, Phys. Rev. Lett. 74 (1995) 4047.
[23] R. Schuster, E. Buks, M. Heiblum, D. Mahalu, V.U.H. Shtrikman, Nature 385 (1997) 417.
[24] Y. Ji, M. Heiblum, D. Sprinzak, D. Mahalu, H. Shtrikman, Science 290 (2000) 779.
[25] Y. Ji, M. Heiblum, H. Shtrikman, Phys. Rev. Lett. 88 (2002) 076601.
[26] M. Büttiker, Phys. Rev. Lett. 57 (1986) 1761.
[27] G. Hackenbroich, Phys. Rep. 343 (2001) 463.
[28] A. Fuhrer, A. Dorn, S. Lüscher, T. Heinzel, K. Ensslin, W. Wegscheider, M. Bichler, Superlattices Microstruct. 31 (2002) 19.
[29] M. Sigrist, A. Fuhrer, T. Ihn, K. Ensslin, W. Wegscheider, M. Bichler, Physica E 2004, in print.
[30] L.P. Kouwenhoven, C.M. Marcus, P.L. McEuen, S. Tarucha, R.M. Westervelt, N.S. Wingreen, in: L.P. Kouwenhoven, G. Schön, L.L. Sohn (Eds.), Nato ASI Conference Proceedings, Kluwer, Dordrecht, 1997, pp. 105–214.
[31] C. Livermore, C.H. Crouch, R.M. Westervelt, K.L. Campman, A.C. Gossard, Science 274 (1996) 1332.
[32] M. Sigrist, A. Fuhrer, T. Ihn, K. Ensslin, W. Wegscheider, M. Bichler, Phys. Rev. Lett. (2004), cond-mat/0307269.
[33] A. Fuhrer, T. Ihn, K. Ensslin, W. Wegscheider, M. Bichler, Phys. Rev. Lett. 91 (2003) 206802.
[34] L. Meier, A. Fuhrer, T. Ihn, K. Ensslin, W. Wegscheider, M. Bichler, Phys. Rev. B 69 (2004) 241302(R).